

Article

Enhanced Integrated Satellite-Terrestrial NOMA with Cooperative Device-to-Device Communication

Michail Karavolos , Nikolaos Nomikos  and Demosthenes Vouyioukas * 

Department of Information and Communication Systems Engineering, School of Engineering, University of the Aegean, 83200 Samos, Greece; mkaravolos@aegean.gr (M.K.); nnomikos@aegean.gr (N.N.)

* Correspondence: dvouyiou@aegean.gr (D.V.)

Received: 9 June 2020; Accepted: 2 September 2020; Published: 7 September 2020

Abstract: The currently deployed terrestrial wireless networks experience difficulties while coping with the massive connectivity demands of coexisting users and devices. The addition of satellite segments has been proposed as a viable way of providing improved coverage and capacity, leading to the formation of integrated satellite-terrestrial networks. In such topologies, non-orthogonal multiple access (NOMA) can further enhance the efficient use of wireless resources by simultaneously serving multiple users. In this paper, an integrated satellite-terrestrial NOMA network is studied where cooperation between ground users is allowed, following the device-to-device (D2D) paradigm. More specifically, the proposed satellite NOMA cooperative (SANOCO) D2D scheme optimally selects pairs of users, by considering the channel conditions of the satellite and the terrestrial D2D links. In SANOCO-D2D users are served through NOMA in the satellite link, and then, if the weak user fails to decode its signal, terrestrial D2D communication is activated to maintain the total sum rate of the system. Comparisons with conventional orthogonal multiple access (OMA) and an alternative NOMA optimal user pairing scheme show that significant sum rate and spectral efficiency gains can be harvested through SANOCO-D2D under varying channel conditions and terrestrial D2D bandwidth.

Keywords: Integrated satellite-terrestrial; NOMA; D2D; cooperative communications

1. Introduction

Future wireless networks will be characterized by dense topologies and diverse services, ranging from high-throughput multimedia applications to ultra-reliable Internet of Things (IoT) communication. The coexistence of both users and devices results in unprecedented hurdles for the currently deployed terrestrial infrastructure. At the same time, aiming to alleviate the stress on terrestrial wireless networks, the integration of satellite and aerial segments has been proposed [1,2]. The efficient cooperation among the terrestrial and space segments enables integrated satellite-terrestrial networks to enjoy improved coverage for both urban and remote areas and increased capacity to serve beyond fifth generation (5G) services. At the same time, the addition of satellites acting as base stations (BSs) in space offers several key benefits to the wireless transmission. More specifically, users can experience improved diversity by connecting to either a terrestrial or satellite BS or both, opportunistically choosing the best possible point for transmission and reception [3].

Another dimension that has been investigated in recent years is the development of spectral efficient multiple access techniques to accommodate the massive connectivity requirements for both users and devices. In this field, non-orthogonal multiple access (NOMA) allows multiple users to share the same resources, thereby avoiding the orthogonal use of wireless channels and its inefficiencies. Since NOMA in the power domain relies on appropriate power allocation, both strong and weak users can be served, maintaining both system throughput and user fairness [4]. An important aspect for

successful NOMA transmissions lies in determining the users that will be paired and share resources. Generally, if two users with asymmetric channel conditions and/or rate requirements are served simultaneously, the sum rate surpasses that of orthogonal multiple access (OMA) [5]. A distributed matching algorithm for optimal power allocation, considering both channel and rate asymmetries, has been proposed by Liang et al. [6] and it was shown to surpass the performance of OMA without incurring high complexity. Further sum rate enhancement can be achieved by employing hybrid schemes where switching between OMA and NOMA takes place in order to allow at least one user to be served when NOMA transmission fails [7].

In the context of integrated satellite-terrestrial networks, the application of NOMA has been suggested to better utilize the wireless resources among the different segments. An overview of NOMA in such topologies has been given in [8], highlighting the advantages of employing NOMA in scenarios, such as cognitive satellite-terrestrial communication and cooperative networks relying on satellite and terrestrial relays. Then, Zhu et al. investigated the downlink communication of ground users with multi-antenna terrestrial BSs and a satellite [9]. More specifically, users were allocated to the satellite according to a channel quality-based scheme, while the remaining users were served by terrestrial BSs through NOMA and paired by solving a max-min problem that maximized their minimum channel correlation. The results revealed a trade-off among fairness and system capacity when the number of users served by the terrestrial BSs increased. The efficient application of NOMA in a two-user network communicating through NOMA with a satellite has been examined by Yan et al. [10]. Towards that end, optimal power allocation was performed for sum rate maximization, while abiding by predetermined target user rates. Additionally, closed-form expressions for the ergodic capacity and the energy efficiency of the system were derived, while performance evaluation showed the superiority of NOMA over OMA. Another work focused on cooperative NOMA (C-NOMA) among two already paired users communicating with a satellite [11]. In greater detail, the strong user forwarded the signal of the weak user when decoding failed at the latter. The performance evaluation in terms of outage probability and ergodic capacity showed the advantage of C-NOMA in the satellite-terrestrial network against time-division multiple access (TDMA)-based OMA. As NOMA relies on user pairs, it is easy to observe that the cooperation between them, in cases where the weak user fails to decode its own message, can lead to robust communication and guaranteed fairness. In various studies, the advantages of device-to-device (D2D) communication have been investigated [12,13]. Thus, the adoption of the D2D communication paradigm opens up tremendous opportunities to further strengthen the performance of integrated satellite-terrestrial NOMA networks, as long as the channel conditions and rate requirements of each pair are jointly considered with the user pairing process of NOMA.

Integrated satellite and terrestrial networks represent an important research topic for 5G and beyond networks and have received several contributions in recent years. Through integrated satellite-terrestrial wireless architectures, multiple wireless systems and access techniques collaborate towards improving the quality-of-service (QoS), coverage and load balancing [14]. At the same time, low Earth orbit (LEO) satellites have been proposed as a viable means for providing additional degrees of freedom for connectivity and data offloading due to reduced latency, compared to other satellite-based solutions with larger distance to the Earth's surface and increased coverage, compared to standalone terrestrial small cells [3,15]. Other works have shown diversity gains by facilitating the cooperation among satellite and terrestrial network segments where users directly transmit and receive to and from the satellite [16]. Moreover, it has been observed that user cooperation in integrated satellite-terrestrial networks, following the D2D paradigm, improves the diversity of the transmission and the performance of spectral-efficient communication techniques, such as NOMA [11]. Finally, from an industrial perspective, the high potential of integrated satellite-terrestrial networks is outlined by the forthcoming plans to deploy dense LEO constellations by OneWeb [17] and SpaceX [18] and cooperate with traditional cellular operators, providing ubiquitous and high QoS communication.

Furthermore, the integration of satellites to complement terrestrial communication provides an interesting trade-off of additional complexity in the architecture, production costs and round-trip delay versus the benefits of improved link quality and coverage. However, it has been shown that the negative aspects of adding a satellite segment are significantly mitigated in the case of LEO satellites. More specifically, the low orbit altitude of LEO satellites, compared to the medium Earth orbit (MEO) and geosynchronous Earth orbit (GEO) satellites, results in one-directional trip delay of less than 14 ms, and a round-trip delay of less than 50 ms being comparable to those of terrestrial links [3]. Furthermore, owing to the small size of satellites and pipeline production, manufacturing costs of LEO satellites are significantly minimized [3,15]. At the same time, the interests of industrial stakeholders in deploying dense LEO constellations highlights the importance of adding more communication segments in the architecture of 5G and beyond networks [17,18]. It is important to note that satellite segments can act in collaboration with other novel propositions, such as spectrum sharing and cognitive radio in order to boost their performance [14].

In this work, we aim at improving the performance of integrated satellite-terrestrial NOMA networks comprising multiple ground users by enabling cooperative D2D communication among them. For this purpose, a pairing scheme for ground users is presented, considering each user's satellite channel, and the terrestrial channels between the users. The objective function of the pairing scheme aims to maximize the system's sum-rate, by evaluating both the satellite segment where NOMA is applied and the terrestrial D2D link between the users that assists the transmission. Specifically, the whole transmission is divided into two phases. In the first transmission phase, the satellite transmits through NOMA towards a pair of users, sharing the same sub-channel, and assigns them a suitable fraction of the total transmit power in order to guarantee that the achievable users' rates are at least equal to those of the conventional OMA. Then, in the second transmission phase, the strong user, i.e., the one with better satellite channel conditions, decodes the weak user signal, and if the D2D link between them provides a higher rate for the weak user than the achievable rate through satellite NOMA, D2D transmission takes place. The main goal of this study is to identify the pairs of users that can benefit from the terrestrial cooperation combined with NOMA in satellite segment, thereby maximizing the total sum rate of the system compared to standalone NOMA. Towards this end, user pairing is modeled as a maximum weighted perfect matching problem in graph theory, considering the achievable rates in the terrestrial and satellite segments. More specifically, in this work, the following contributions are provided:

- A novel user pairing scheme is proposed, considering the satellite channels and the terrestrial D2D channels. In order to study this problem, graph theory is invoked—modeling it as a maximum weighted perfect matching problem.
- Power allocation for NOMA in each transmission period considers the achieved rates through orthogonal multiple access (OMA). In this way, the proposed power allocation guarantees that user pairing will lead to a higher rate for each pair member and an overall rate increase for the network.
- The impact of various system parameters inherent to satellite-based access and D2D networks have been evaluated, i.e., the elevation angle and the bandwidth allocation, respectively. As a result, guidelines are given in order to achieve improved satellite-terrestrial cooperation and spectral efficiency, compared to standalone NOMA and OMA deployments.

The structure of the paper is as follows. Section 2 presents the system model, while Section 3 provides the details of SANOCO-D2D scheme. Next, performance evaluation is conducted in Section 4. Finally, conclusions and future directions are given in Section 5.

2. System Model

2.1. Topology

A network consisting of a LEO satellite and $N = 2K$ user equipment (UEs) located in a circle with radius R and within the LEO satellite coverage area is considered, as depicted in Figure 1. The UEs can communicate with the satellite and with each other via D2D links. The satellite is equipped with an antenna with transmitting gain G_t^s and total available transmit power P_s . Additionally, the satellite downlink frequency operates at a frequency f_s and the total available bandwidth is denoted as B_s . Furthermore, each UE_i has three antennas, one for the reception of the satellite signal with a reception gain denoted as G_r^s and two antennas for the transmission and the reception of the terrestrial signal to and from other devices that are located within the area of interest and with gains G_t^d and G_r^d , respectively. The operating frequency for the terrestrial D2D links is denoted as f_d and the total available bandwidth as B_d . Besides, each UE_i has a maximum available transmit power P_d and the receiver equipment for the satellite and the terrestrial D2D signals have noise temperatures denoted as T_s and T_d , respectively.

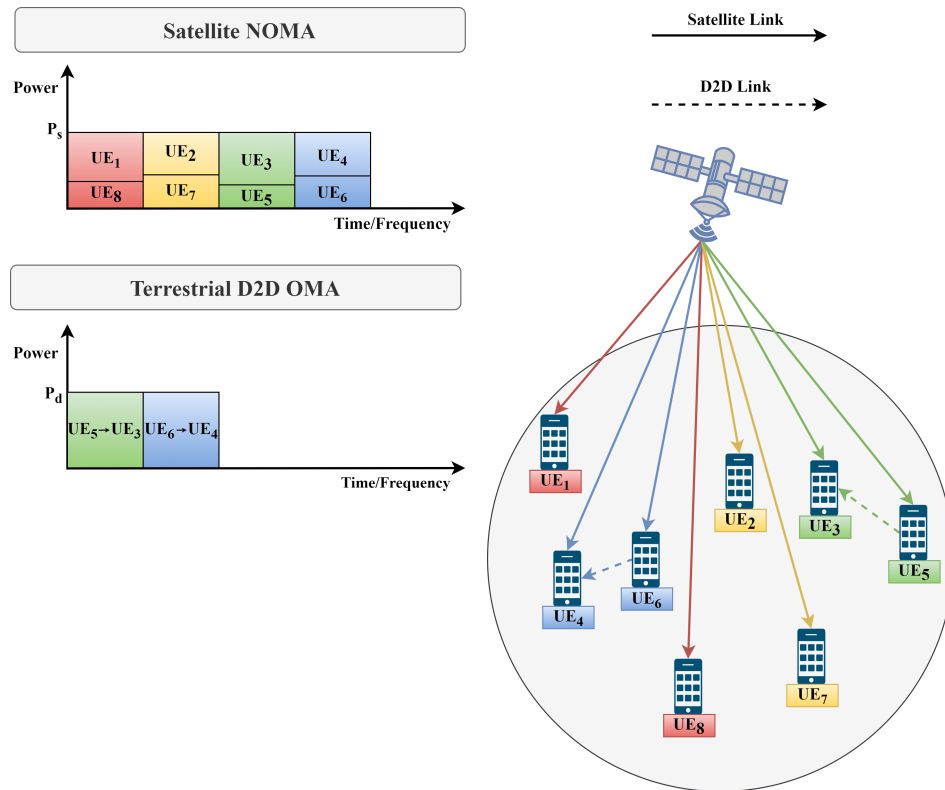


Figure 1. System model with $N = 8$ user equipment (UEs).

UEs are served through a satellite-aided and cooperative D2D network where the satellite is mainly responsible for the communication, while the D2D scheme is employed between the devices to improve the total communication quality. The communication with the UEs is divided into two phases. During the first transmission phase, the satellite employs NOMA based on a user pairing policy in the power domain to transmit the data to pairs of UEs using superposition coding, as illustrated in Figure 1. Practically, the satellite takes into account the channel conditions of each UE_i regarding the satellite link and the channel conditions of terrestrial D2D links between each UE_i and UE_j pair where $i \neq j$, and applies user pairing. Each pair of UEs will share the same sub-channel in the frequency/time domain and within this sub-channel, a power allocation scheme will take place to assign different power levels to each UE_i . During the second phase, the UEs with favorable satellite

channel conditions from each pair decode the received satellite signal and transmit the decoded signal via a D2D communication link to their pair. Thus, the UEs with weak channel conditions towards the satellite will have two copies of their own signal in the power domain and will select the best one in order to achieve the maximum rate. On the other hand, the UEs with strong channel conditions towards the satellite, perform successive interference cancellation (SIC) and get their own signals. Terrestrial communication between D2D pairs takes place over the time/frequency domain using OMA. Hence, each D2D pair communicates in a different sub-channel without interfering with D2D links of neighboring pairs, as illustrated in Figure 1.

2.2. Channel Model

The fading environment for the land mobile satellite (LMS) channel is modeled through the Loo's model distribution [19], where the power of the line of sight (LoS) component is log-normally distributed with parameters (M, Σ) , while the power of the multipath component (MP) follows the Rayleigh distribution with the complex channel coefficients being represented by h_i^s for each UE_i, assuming zero mean and variance:

$$\sigma_s = \sqrt{0.5 \cdot 10^{\frac{MP}{10}}} \sim \mathcal{N}(0, \sigma_s^2). \quad (1)$$

Furthermore, pathloss attenuation using the free space pathloss (FSL) model is considered, being denoted as L_{FS_i} for each UE_i. In addition, a maximum Doppler shift of 40 kHz is assumed and modeled with the Jakes model [20].

Regarding the terrestrial D2D links, the multipath fading is modeled by the Rayleigh distribution with zero mean and unit variance $\sim \mathcal{N}(0, 1)$. The complex channel coefficient is $h_{i,j}^d$ for each D2D pair of UE_i and UE_j. Additionally, log-normal shadowing is considered with zero mean and variance σ_λ^2 with $\sim \mathcal{N}(0, \sigma_\lambda^2)$. Furthermore, pathloss attenuation of the D2D links, denoted as $PL(d)_{i,j}$ and expressed in dB for a pair of users being d km apart from each other, is modeled as in [21]:

$$PL(d)_{i,j} = 127 + 30 \log_{10}(d). \quad (2)$$

Moreover, the LMS and terrestrial D2D links are degraded by additive white Gaussian noise (AWGN) $\sim \mathcal{N}(0, \sigma^2)$. The noise power is calculated as the product of the Boltzmann constant k , the receiver system noise temperature T_g , ($g = \{s, d\}$) and the available bandwidth B_s and B_d . Thus, the noise power of the satellite and terrestrial receivers is equal to $N_s = kT_s B_s$ and $N_d = kT_d B_d$, respectively. Consequently, the corresponding variances for each receiver type are equal to $\sigma_s = \sqrt{N_s}$ and $\sigma_d = \sqrt{N_d}$.

2.3. Transmission Parameters and Achievable Rates

In case that the satellite applies the NOMA scheme based on user pairing, for each pair of users, the satellite transmits a superimposed signal as:

$$x_s = \sqrt{G_t^s} \left(\sqrt{\alpha_i P_s} s_i + \sqrt{\alpha_j P_s} s_j \right). \quad (3)$$

where s_i and s_j are the signals for the users UE_i and UE_j, respectively, and α_i and α_j denote the fraction of the total satellite transmit power P_s that is assigned to each user, with $\alpha_i + \alpha_j = 1$. Then, each UE_l with $l = \{i, j\}$ receives the satellite signal:

$$y_l^s = \sqrt{\frac{G_r^s}{L_{FS_l}}} h_l^s x_s + z_n^s, \quad (4)$$

where z_n^s is the AWGN noise in the satellite link. The channel gain Γ_l for each UE_{*l*} including additional gains, losses and the noise power of the satellite receiver N_s is given as:

$$\Gamma_l = \frac{G_t^s G_r^s}{L_{FS_l} N_s} |h_l^s|^2. \quad (5)$$

Assume that UE_{*i*} and UE_{*j*} form a pair with $\Gamma_i \leq \Gamma_j$. Thus, the UE_{*j*} is the strong channel satellite user and UE_{*i*} is the weak channel satellite user. According to the NOMA principle, the fraction of the total satellite transmit power assigned to UE_{*j*} should be less than the fraction of the power assigned to UE_{*i*} i.e., $a_j \leq a_i$. As a result, UE_{*j*} performs SIC and decodes their signal s_j . At the same time, the weak channel satellite user UE_{*i*} directly decodes the s_i , and s_j is treated as noise. Thus, the achievable rates for each UE_{*i*} and UE_{*j*} that form a pair in a satellite sub-channel are given from the following equations:

$$R_j^{NOMA(i,j)} = B_c^{NOMA} \log_2 (1 + \alpha_j P_s \Gamma_j), \quad (6)$$

$$R_i^{NOMA(i,j)} = B_c^{NOMA} \log_2 \left(1 + \frac{(1 - \alpha_j) P_s \Gamma_i}{\alpha_j P_s \Gamma_i + 1} \right), \quad (7)$$

where B_c^{NOMA} is the satellite channel bandwidth in the case of NOMA. In particular, when the satellite applies NOMA, user pairing allocates to each pair a sub-channel on the satellite and within this sub-channel different power allocation factors are assigned to each user of the pair. Therefore, the total number of sub-channels in this case is equal to $N/2$ and the total available satellite bandwidth is equally distributed to each sub-channel. Thus, the satellite channel bandwidth for NOMA is equal to $B_c^{NOMA} = 2B_s/N$.

On the contrary, for OMA, each user is allocated a separate channel. Thus, the available satellite bandwidth is equally assigned to each UE_{*k*}. As a result, the channel bandwidth in this case is equal to the channel bandwidth in case of NOMA, multiplied by 1/2, i.e., $B_c^{OMA} = B_c^{NOMA}/2$, and the achievable rate for each UE_{*k*} is given as:

$$R_k^{OMA} = \frac{1}{2} B_c^{NOMA} \log_2 (1 + P_s \Gamma_k). \quad (8)$$

Regarding the terrestrial communication, the channel gain for the D2D link $\Lambda_{i,j}$ between UE_{*i*} and UE_{*j*}, including the channel coefficient $|h_{i,j}^d|^2$, additional gains, losses and the noise power of the terrestrial receiver N_d , is modeled as:

$$\Lambda_{i,j} = \frac{G_t^d G_r^d}{PL(d)_{i,j} N_d} |h_{i,j}^d|^2, \quad (9)$$

where $PL(d)_{i,j}$ is equal to the antilogarithm of the result that is calculated via (2). The achievable rate for UE_{*i*} through the D2D link with UE_{*j*} it is equal to:

$$R_i^{D2D(i,j)} = B_c^{D2D} \log_2 (1 + P_d \Lambda_{i,j}), \quad (10)$$

where B_c^{D2D} is the channel bandwidth that is allocated to a pair of users forming a terrestrial D2D link. Since D2D communication between a pair of users takes place in a different sub-channel, we do not take into account interference between the satellite and the D2D links. The total bandwidth for D2D OMA communication is equally allocated to the total number of pairs and is equal to $N/2$. Thus, the channel bandwidth that allocated to a pair of users with regard to the corresponding D2D link is equal to $B_c^{D2D} = 2B_d/N$. Also, it is noteworthy that the achievable rate for user UE_{*j*} is equal to the achievable rate for user UE_{*i*} in case of a D2D link $R_i^{D2D(i,j)} = R_j^{D2D(i,j)}$.

Finally, concerning the CSI reporting procedure, pilot symbols are sent from the satellite, prompting the UEs to estimate their satellite link CSI. Simultaneously, UEs transmit pilot symbols, enabling UEs within their coverage to estimate their D2D channel conditions. In the next step, the satellite receives the CSI of the satellite and D2D links, and while acting as a central node, executes SANOCO-D2D. It should be noted that the UEs are able to identify whether the D2D link is profitable compared to standalone optimal NOMA user pairing, by comparing the corresponding achievable rates. If a D2D link between a pair of users is not profitable, it is an outage, so UEs notify the satellite. After that, the satellite notifies the UEs about the formed pairs and whether or not the D2D link will be used. Moreover, retransmissions rely on an Acknowledgment/Negative-Acknowledgment (ACK/NACK) mechanism, where the UEs broadcast short-length error-free packets via a separate narrow-band link, informing the network on whether or not the packet transmission was successful.

3. Satellite-Aided NOMA with Cooperative D2D Communication

In this section, details on the proposed satellite-aided NOMA with cooperative D2D (SANOCO-D2D) scheme are given. Moreover, in order to better illustrate the SANOCO-D2D technique, a toy network is presented.

3.1. SANOCO-D2D Operation

At the start of each transmission phase, UE_i reports its CSI to the satellite that estimates the channel coefficient $|h_i^s|^2$ and calculates the channel gain Γ_i using (5). Moreover, the channel gain for the D2D link $\Lambda_{i,j}$ is calculated between each UE_i , UE_j pair, using the reported channel coefficient $|h_{i,j}^d|^2$ via (9). Next, the satellite applies NOMA based on user pairing and calculates the power allocation factors for each pair by solving the following maximization problem:

$$\begin{aligned} \max_{\alpha_j} \quad & R_i^{\text{NOMA}(i,j)} + R_j^{\text{NOMA}(i,j)}, \\ \text{s.t.} \quad & R_i^{\text{NOMA}(i,j)} \geq R_i^{\text{OMA}}, \\ & R_j^{\text{NOMA}(i,j)} \geq R_j^{\text{OMA}}, \\ & 0 \leq \alpha_j \leq 1. \end{aligned} \quad (11)$$

Essentially, the solution to the maximization problem (11) is the optimal power allocation factor α_j for the strong user UE_j that maximizes the sum rate and guarantees that the achievable rate of users through NOMA will not be less than the achievable rate of OMA. Since $\Gamma_i \leq \Gamma_j$, the optimal power allocation factor α_j of the strong user UE_j is given as in [6]:

$$\alpha_j = \frac{\sqrt{1 + \Gamma_i P_s} - 1}{\Gamma_i P_s}. \quad (12)$$

It is important to note that the achievable rate of the weak satellite user $R_i^{\text{NOMA}(i,j)}$ under optimal power allocation is equal to the R_i^{OMA} . Thus, the power allocation factor for the weak satellite user should satisfy the rate constraint for this user, while allocating all the remaining power to the strong satellite user to maximize the achievable sum rate.

An important element of SANOCO-D2D is the possibility of D2D communication when the weak user is not able to decode its message through NOMA. In this case, the strong satellite user UE_j is responsible for transmitting the received signal from the satellite to the weak satellite user UE_i . Due to the use of NOMA at the satellite, UE_j decodes the signal of weak user UE_i and acts as a relay to forward it to its destination. Therefore, the weak satellite user UE_i will have two copies of its own signal and

selects the best one in order to maximize its achievable rate. For the strong user, the achievable rate of the weak user's signal is equal to:

$$R_i^{DECODED(i,j)} = B_c^{NOMA} \log_2 \left(1 + \frac{(1 - \alpha_j)P_s\Gamma_j}{\alpha_j P_s \Gamma_j + 1} \right). \quad (13)$$

The achievable rate of UE_i that will be served via D2D cooperation with UE_j is given by:

$$R_i^{NOMA-D2D(i,j)} = \min \left(R_i^{D2D(i,j)}, R_i^{DECODED(i,j)} \right). \quad (14)$$

The total sum rate of the UE_i and UE_j pair is calculated as:

$$R_{i,j} = R_j^{NOMA(i,j)} + \max \left(R_i^{OMA}, R_i^{NOMA-D2D(i,j)} \right), \quad (15)$$

where $\max \left(R_i^{OMA}, R_i^{NOMA-D2D(i,j)} \right)$ is the rate that the weak user UE_i is able to achieve using the proposed cooperative technique.

Remark 1. It is noteworthy that in the worst case in which the D2D channel between the two users is not profitable, i.e., $R_i^{D2D(i,j)} \leq R_i^{OMA}$, the weak user will select to retrieve its data from the received satellite signal, maintaining the rate of each user and the total sum rate as in [6]. On the contrary, if $R_i^{D2D(i,j)} > R_i^{OMA}$, the weak user will retrieve its data from the received signal through the D2D link, achieving a higher rate than R_i^{OMA} , significantly benefiting the total sum rate compared to the result in [6].

Remark 2. In cases where D2D communication is highly profitable, i.e., $R_i^{D2D(i,j)} \geq R_i^{DECODED(i,j)}$, the weak user is able to achieve the maximum rate of $R_i^{DECODED(i,j)}$. As a result, the total sum rate will be equal to $R_{i,j} = B_c^{NOMA} \log_2 (1 + \alpha_j P_s \Gamma_j) + B_c^{NOMA} \log_2 \left(1 + \frac{(1 - \alpha_j)P_s\Gamma_j}{\alpha_j P_s \Gamma_j + 1} \right) \Rightarrow R_{i,j} = B_c^{NOMA} \log_2 (1 + P_s \Gamma_j)$, as all quantities will be positive. Thus, in the proposed scheme, the total sum rate is bounded as $R_j^{NOMA(i,j)} + R_i^{OMA} \leq R_{i,j} \leq B_c^{NOMA} \log_2 (1 + P_s \Gamma_j)$. In conclusion, the maximum sum rate will be equal to the case where only the strong user is connected to the satellite, while the upper bound for the rate of the weak user UE_i will be equal to $R_i^{DECODED(i,j)}$ and the lower bound will be equal to R_i^{OMA} .

So far, we have analyzed the proposed technique for an arbitrary UE pair. Since the network consists of $N = 2K$ users, the main goal is to maximize the total sum rate of the system. Therefore, a matching scheme between terrestrial users must take place in order to identify those user pairs that maximize the total sum rate of the system. Towards this end, SANOCO-D2D considers both the channel between the satellite and each user of the system and the terrestrial D2D channel among the possible user pairs. For this purpose, it is necessary to define a binary matrix \mathbf{U} that presents the pairing relationship between the users:

$$u_{i,j} = \begin{cases} 1 & \text{UE}_i \text{ pairs UE}_j, \\ 0 & \text{otherwise.} \end{cases} \quad (16)$$

The diagonal elements of the pairing matrix \mathbf{U} are equal to zero because one user cannot pair itself. Furthermore, it can be easily observed that $u_{i,j} = u_{j,i}$, because if user UE_i forms a pair with UE_j, then $u_{i,j} = 1$, and of course, the pair of UE_j is user UE_i; thus, $u_{j,i} = 1$. The following maximization problem describes the proposed scheme for the whole network:

$$\begin{aligned}
 \max_{u_{i,j}} \quad & \sum_{i=1}^N \sum_{j=i+1}^N u_{i,j} R_{i,j}, \\
 \text{s.t.} \quad & \sum_{j=1}^{i-1} u_{j,i} + \sum_{j=i+1}^N u_{i,j} = 1, \quad \forall i \in \{1, \dots, N\}, \\
 & u_{i,j} \in \{0, 1\}, \quad 1 \leq i, j \leq N.
 \end{aligned} \tag{17}$$

Practically, the value of the objective function at the optimal solution of the maximization problem (17) is the maximum sum rate, denoted as R_{\max} , of the system. The first constraint of the maximization problem states that each user can pair with exactly one other user.

The maximization problem (17) is an integer programming problem which is hard to solve. In order to solve this problem efficiently, a weighted matching graph $G = (V, E)$ is created, where the total number of vertices is equal to the total number of users $|V| = N$. Thus, each vertex $v_i \in V$ represents the corresponding user UE_i . Moreover, each vertex v_i with $i = \{1, \dots, N\}$ is connected to all the other vertices that is not already connected $v_j \in V$ with $i \neq j$ and $j = \{1, \dots, N\}$, forming the edge $e_{i,j} \in E$ with weight $w_{i,j}$ that represents a possible pairing of UE_i and UE_j . G is an undirected graph in which edge $e_{i,j}$ exists and there is no existence of the backward edge $e_{j,i}$, so the total number of edges equals $|E| = \binom{N}{2} = N(N - 1)/2$, which is the choice of two users by N total users. For each edge of the graph, the connection of the corresponding vertices are defined as:

$$e_{i,j} = \begin{cases} 1 & v_i \text{ is connected to } v_j \\ 0 & v_i \text{ is not connected to } v_j \end{cases} \tag{18}$$

Regarding the proposed technique, the $w_{i,j} = R_{i,j}$, which is the total sum rate that pair of users UE_i and UE_j can achieve and is always positive. Thus, the maximization problem (17) is modified, as a maximum weighted matching problem in graph theory and specifically perfect, because each user will match with exactly one other user, which can be solved optimally by the Edmonds algorithm [22] in polynomial time. The Edmonds algorithm can be implemented in time $O(|V|^3)$ [23,24], and faster implementation with time complexity $O(|V||E|\log|V|)$ was given in [25]. Algorithm 1 shows the procedure that is followed in order to create the maximum weighted matching graph.

Algorithm 1: Graph creation.

```

1 Input: Total number of UEs  $N$ ;
Result:  $G = (V, E)$ 
2 for  $i \leftarrow 1$  to  $N$  do
3   Add vertex  $v_i$  to  $G$ ;
4    $V = V + v_i$ ;
5 end
6 for  $i \leftarrow 1$  to  $N$  do
7   for  $j \leftarrow i + 1$  to  $N$  do
8     Connect vertices  $v_i$  and  $v_j$  with and edge  $e_{i,j}$  in  $G$ ;
9     Set initial weight of the edge  $e_{i,j}$  to  $w_{i,j} = 0$ ;
10     $E = E + e_{i,j}$ ;
11  end
12 end

```

Regarding the operations that should be performed during the execution of Algorithm 1, at first, the total number of users N is given as an input and the vertices of the graph which represent the UEs in the system are created. Thus, for each UE_i with $(1 \leq i \leq N)$ a corresponding vertex v_i is

created and added to the graph G and to the set of vertices V . After that, each vertex of the graph should be connected with all the other vertices in the graph that is not already connected. For this reason, the algorithm visits the vertex v_i with $(1 \leq i \leq N)$ and connects this vertex with all the other vertices v_j of the graph with $(i < j \leq N)$ via a properly labeled edge $e_{i,j}$ with initial weight $w_{i,j} = 0$. Additionally, the new edge $e_{i,j}$ with weight $w_{i,j}$ should be added to the set of edges E of the graph. When the edge creation procedure terminates, Algorithm 1 gives as an output the graph structure that will be used for this specific number of UEs N in order to update the weights of each edge and solve the maximum weighted matching problem using the Algorithm 2 and the Edmonds algorithm. In this way, SANOCO-D2D can model all the possible pair of users that are able to be formed and served only from the satellite via NOMA or via NOMA and D2D, when the D2D link does not experience failures, and at the same time, it is characterized as profitable compared to standalone satellite NOMA. Note that Algorithm 1 is executed once at the beginning for a specific number of users and also it is possible to save the structure of the graph for different numbers of users and re-load it whenever the number of users in the system changes.

The steps of SANOCO-D2D for maximizing the sum rate of the system are given in detail in Algorithm 2.

Algorithm 2: SANOCO-D2D.

```

1 Input: Satellite CSI for each UEi and CSI between all the UEi and UEj;
2 for  $i \leftarrow 1$  to  $N$  do
3   for  $j \leftarrow i + 1$  to  $N$  do
4     Find which is the strong and the weak channel satellite user for each pair by comparing
      the corresponding channel gains  $\Gamma_i$  and  $\Gamma_j$ ;
5     Derive the power allocation factor  $\alpha_t$  for the strong channel satellite user through (12);
6     Calculate the achievable rate  $R_{\text{strong}}^{\text{NOMA}(i,j)}$  of the strong user using (6);
7     Calculate the achievable rate  $R_{\text{weak}}^{\text{OMA}}$  of the weak user using (8) which is achieved under
      the satellite NOMA optimal power allocation;
8     Calculate the rate  $R_{\text{weak}}^{\text{D2D}(i,j)}$  that the weak satellite user is able to achieve via the
      corresponding D2D link  $i \rightarrow j$  through (10);
9     Calculate the rate  $R_{\text{weak}}^{\text{DECODED}(i,j)}$  that the weak user is able to achieve in case that the
      strong user decode their signal using (13);
10    Calculate the achievable rate of the weak user regarding the D2D link, taking into
      account the rates  $R_{\text{weak}}^{\text{D2D}(i,j)}$  and  $R_{\text{weak}}^{\text{DECODED}(i,j)}$  from (14);
11    Derive the total sum rate  $R_{i,j}$  that this possible pair of users are able to achieve through
      (15);
12    Set the weight  $w_{i,j}$  of the edge  $e_{i,j} \in E$  of the graph  $G$  to  $w_{i,j} = R_{i,j}$ ;
13  end
14 end
15 Output: Optimal user pairing policy  $\mathbf{u}_{i,j}^*$  and the maximum sum rate  $R_{\max}$ 

```

Algorithm 2 presents the procedure SANOCO-D2D for maximizing the total sum rate of the system. The algorithm takes as an input the CSI of the satellite link of each user, and the CSI of each D2D link between the users. Next, it updates the weights of the edges of the graph G that has been created during the execution of Algorithm 1. Specifically, the algorithm visits each vertex v_i with $(1 \leq i \leq N)$ of the graph representing each UE_i, and calculates and assigns an appropriate weight $w_{i,j}$ to each edge $e_{i,j}$ connecting this vertex with the vertex v_j of the graph with $(i < j \leq N)$. Obviously, when the algorithm visits vertex v_N , the procedure of updating the weights of the edges of the graph

immediately terminates, because all the weights of the edges connecting vertex v_N with all the other vertices of the graph G have been updated during the previous iterations.

With the proposed algorithm, in order to calculate the weight $w_{i,j}$ that should be assigned to the edge $e_{i,j}$ connecting vertices v_i and v_j with ($i < j$) and indicate a possible pair of users, the identification of the strong and the weak satellite users should be performed first, by comparing the corresponding channel gains Γ_i and Γ_j of UE_i and UE_j that are modeled as the vertices v_i and v_j of the graph G . Then, the calculation of the power allocation factor of the strong satellite user takes place using (12). Subsequently, using (6) the achievable rate $R_{\text{strong}}^{\text{NOMA}(i,j)}$ of the strong satellite user is calculated in the context of NOMA optimal user pairing scheme. Thereafter, via (8), the achievable rate $R_{\text{weak}}^{\text{OMA}}$ of the weak satellite user under the satellite NOMA optimal power allocation scheme should be calculated. Keep in mind that the achievable rate of the weak satellite user $R_{\text{weak}}^{\text{NOMA}(i,j)}$ under optimal power allocation is equal to $R_{\text{weak}}^{\text{OMA}}$ because the power allocation factor that is assigned to the weak satellite user should satisfy the rate constraint for this user, while all the remaining power is allocated to the strong satellite user in order to maximize the achievable system sum rate.

In the next step, the algorithm calculates the rate $R_{\text{weak}}^{\text{D2D}(i,j)}$ that the weak satellite user is able to achieve via the corresponding D2D link if this pair is used, through (10), and the rate $R_{\text{weak}}^{\text{DECODED}(i,j)}$ that the weak user is able to achieve in case that the strong user forwards the received signal from the satellite to the weak user using (13). Next, considering the rate $R_{\text{weak}}^{\text{D2D}(i,j)}$ that the D2D link is able to offer to the weak user, and the rate $R_{\text{weak}}^{\text{DECODED}(i,j)}$ that the weak user is able to achieve when the strong user forwards the weak user signal, the algorithm calculates the achievable rate of the weak user by calculating the minimum of these two rates through (14), and practically uses this information to identify whether or not the D2D link is preferable compared to the directly received coded satellite signal at the weak user. Here note that the algorithm must calculate the minimum of $R_{\text{weak}}^{\text{D2D}(i,j)}$ and $R_{\text{weak}}^{\text{DECODED}(i,j)}$, because if the D2D rate surpasses the achieved rate of the weak user's signal at the strong user, then the strong user is able to send the weak user's signal through the D2D channel without errors. On the contrary, if the achievable rate regarding the D2D link is less than the rate of the weak users signal that received from the satellite at the strong user, then the D2D rate is a bottleneck that will result in reduced rate. In other words, the minimum of the two rates represents the total profit or loss of D2D cooperation.

As a final step, for the weight update procedure of $e_{i,j}$, the algorithm calculates the total sum rate that this pair of users is able to achieve through (15). The first term on the right hand side of (15) represents the achievable rate of the strong satellite user using the NOMA optimal user pairing scheme, while the second term is the achievable rate of the weak user. The achievable rate of the weak satellite user is calculated by applying the maximum function between the achievable rate $R_{\text{weak}}^{\text{OMA}}$ of the weak user using the NOMA optimal user pairing scheme at the satellite and the achievable rate of the weak user $R_{\text{weak}}^{\text{NOMA-D2D}(i,j)}$ through the D2D link. In this way, it is ensured that if a D2D link failure occurs; then the weak channel satellite user will be served only through NOMA. Next, the weight $w_{i,j}$ of the edge $e_{i,j}$ is updated to the value that was calculated in the previous step through (15). The weight $w_{i,j}$ of the edge $e_{i,j}$ indicates the sum rate that this possible pair of users UE_i and UE_j is able to achieve and contributes to the total sum rate of the system. Finally, when the procedure of weight updating terminates, the Edmonds algorithm is executed, giving as an output the optimal user pairing policy $u_{i,j}^*$ and the maximum sum rate R_{\max} of the system.

The proposed scheme considers the possibility where in some cases, the D2D link between two users may not be feasible because of power or propagation issues, and thus the weak user is only served through the satellite. Thus, if no profitable D2D link exists, then the optimal user pairing policy and the maximum sum rate coincide with the optimal downlink user pairing NOMA scheme [6].

3.2. Toy Network

Following the operation of Algorithm 1, a network consisting of $N = 4$ UEs is assumed, and so, four vertices are created, where $v_1 = \text{UE}_1$, $v_2 = \text{UE}_2$, $v_3 = \text{UE}_3$ and $v_4 = \text{UE}_4$, and added to the set of vertices V . Next, starting from UE₁, the algorithm connects this vertex with all the other three vertices using appropriate edge labeling, by initially setting the weight of each edge to zero. Thus, through this step, the vertex UE₁ is connected with the vertex UE₂ via the edge $e_{1,2}$, with the vertex UE₃ via the edge $e_{1,3}$ and with the vertex UE₄ via the edge $e_{1,4}$. The weights $w_{1,2} = w_{1,3} = w_{1,4} = 0$ of the corresponding edges are initially set to zero and all edges are added to the set of edges E of the graph G . Thereafter, the algorithm visits the next vertex, i.e., UE₂ and connects it with vertices UE₃ and UE₄ via the edges $e_{2,3}$ and $e_{2,4}$, where again, the weights are set to zero $w_{2,3} = w_{2,4} = 0$. Obviously, the edge $e_{1,2}$ that connects the vertex UE₁ with the vertex UE₂, indicating the formation of a possible pair of users, has been already created and added to the set of edges E during the previous step, and there is no need to create it again. After that, the algorithm visits the vertex UE₃ and connects this vertex with the vertex UE₄ via the edge $e_{3,4}$ and set the weight $w_{3,4} = 0$ of this edge to zero. Finally, Algorithm 1 visits the last vertex UE₄ and terminates because this vertex has been already connected with all the other vertices of the graph G .

In Figure 2, the graph setup that is produced through the execution of Algorithm 1 with $N = 4$ UEs is illustrated. The total number of vertices is equal to the total number of users $|V| = 4$ and the total number of edges is equal to $|E| = 6$. Each edge $e_{i,j}$ has a weight $w_{i,j}$ with $i < j$, initially being equal to zero. Using (16) and (18), if the solution that gives the maximum sum rate through Algorithm 2 connects vertices v_i and v_j , UE_i and UE_j will form a pair and $e_{i,j} = 1$. Otherwise, vertices v_i and v_j are not connected and $e_{i,j} = 0$.

It should be noted that the full mesh network presented in Figure 2 is not the optimal user pairing policy that gives the maximum sum rate of the system, but the graph setup that is created once for this specific number of users ($N = 4$) through Algorithm 1, representing all the possible pairs of users with their corresponding achievable rates, indicated as a weight of the corresponding edge. Practically the graph illustrated in Figure 2 is an input for the maximum weighted perfect matching problem that is adopted by SANOCO-D2D, and the solution of this problem keeps only the edges from the optimal pair of users $\mathbf{u}_{i,j}^*$ that gives the maximum sum of weights (maximum sum rate R_{\max}) with the constraint that each vertex must be connected with exactly one other vertex in the graph, thereby ensuring that each user will be paired with exactly one other user in the system in order to perform NOMA or NOMA-D2D transmission, i.e., SANOCO-D2D.

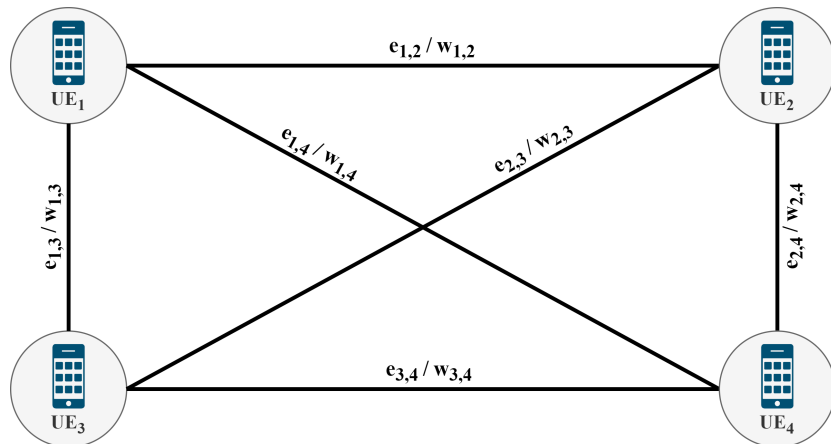


Figure 2. An illustrative example of the graph setup that is used by the proposed technique in order to find the optimal user pairing policy $\mathbf{u}_{i,j}^*$ and the maximum sum rate R_{\max} for $N = 4$ UEs.

Once the graph setup that is shown in Figure 2 is created or loaded for the case of $N = 4$ UEs, the execution of Algorithm 2 starts. Algorithm 2 receives as an input the CSI of each user regarding the channel condition with the satellite, and the D2D CSI between all users. The algorithm starts with the edge weight update procedure by visiting first the vertex UE₁, while updating for each edge $e_{1,j}$, the weight $w_{1,j} = R_{1,j}$ of the corresponding edge with $j = \{2, 3, 4\}$, following the steps of Algorithm 2. In this way, the weight $w_{1,j}$ of each edge $e_{1,j}$ indicates the pair rate that this pair of users UE₁ and UE_j is able to achieve and contribute to the total system sum rate. Next, the algorithm visits the vertex UE₂ and by following exactly the same procedure, updates for each edge $e_{2,j}$ the corresponding weight $w_{2,j} = R_{2,j}$ using the calculated pair rate $R_{2,j}$ for this pair of users, with $j = \{3, 4\}$. The edge weight update procedure terminates when the algorithm visits vertex UE₃ and updates the weight $w_{3,4} = R_{3,4}$ of the edge $e_{3,4}$ to be equal with the calculated pair rate $R_{3,4}$ for this pair of users UE₃ and UE₄. Now, through the weight update procedure, each edge of the graph G , representing a possible pair, has a positive weight value indicating the achievable sum rate for each possible pair.

As a final step, in order to identify the optimal user pairing policy \mathbf{u}_{ij}^* and the maximum system sum rate R_{\max} , graph $G = (E, V)$ with the updated weight values is fed to the Edmonds algorithm which solves the maximum weighted perfect matching problem. As a result, the pair of users maximizing the system sum rate is derived. As a trivial example, consider that $w_{1,2} = 3$, $w_{1,3} = 7$, $w_{1,4} = 1$, $w_{2,3} = 2$, $w_{2,4} = 5$ and $w_{3,4} = 4$. In Table 1, the different possible pairs of users that can be formed with $N = 4$ UEs, and the achievable system sum rate of each possible formation in the system are presented.

Table 1. An example of the different possible pairs and the corresponding achievable system sum rate for the possible formations with $N = 4$ UEs.

Possible Formed Pairs	System Sum Rate
$P_{1,2} = \{\text{UE}_1, \text{UE}_2\}$ and $P_{3,4} = \{\text{UE}_3, \text{UE}_4\}$	$w_{1,2} + w_{3,4} = 7$
$P_{1,3} = \{\text{UE}_1, \text{UE}_3\}$ and $P_{2,4} = \{\text{UE}_2, \text{UE}_4\}$	$w_{1,3} + w_{2,4} = 12$
$P_{1,4} = \{\text{UE}_1, \text{UE}_4\}$ and $P_{2,3} = \{\text{UE}_2, \text{UE}_3\}$	$w_{1,4} + w_{2,3} = 3$

As it can easily be observed from Table 1, if UE₁ is paired with UE₃, and at the same time, UE₂ is paired with UE₄, the maximum system sum rate $R_{\max} = w_{1,3} + w_{2,4} = 12$ is achieved and those pairs constitute the optimal user pairing policy. This is the optimal formation of the pairs that the Edmonds algorithm gives as a solution to the maximum weighted matching problem, and the maximum sum rate. The graph with the formed pairs maximizing the sum rate for this toy network, is illustrated in Figure 3.

The possible formed pairs that are presented in Table 1 are unique, because it is not allowed for a vertex in the graph to be unconnected, and at the same time, it is not allowed for an edge to start and end to the same vertex. Furthermore, exactly one edge is allowed to be connected at each vertex of the graph. In other words, each user should form a pair with exactly one other user of the system and it is not allowed to pair itself or to remain unpaired.

Finally, it should be noted that during the weight update procedure of Algorithm 2, if D2D communication is not profitable or it is not feasible due to link failures, the result shown in Figure 3 concerning the optimal user pairing policy will be exactly the same as in the case of the downlink NOMA optimal user pairing technique [6]. In conclusion, it is possible that some pairs will cooperate via D2D links and some others will not, which is the philosophy behind SANOCO-D2D. As it will be discussed below, D2D cooperation can provide substantial gains for the sum rate of the system and the spectral efficiency.



Figure 3. Optimal user pairing policy $u_{i,j}^*$ that gives the maximum sum rate R_{\max} for $N = 4$ UEs and the studied toy network.

4. Performance Evaluation

In this section, simulation results are presented in terms of sum rate and spectral efficiency for different system parameters and transmission techniques. The whole transmission takes place in an urban terrestrial environment. Towards this end, a custom made simulator was implemented in C++. Furthermore, the maximum weighted perfect matching problem was solved with the use of the LEMON graph library [26]. The average Loo model channel parameters (M, Σ, MP) were selected based on the Table XIII of [27] and are presented in Table 2 for an urban area, operating in the L-Band and handheld antennas. Regarding the satellite channel conditions with terrestrial users, it should be noted that in urban areas, users being a few meters away may experience different channel conditions because of trees, roads, moving vehicles and buildings with different heights acting as scatters and affecting LoS connectivity [27,28]. All users in our scenario have the same elevation angle and range from and to the satellite but experience different channel conditions (LoS), including intermediate and deep shadowing as presented in Table 2, thereby representing the complex nature of an urban environment. On the contrary, in suburban or rural areas the channel conditions of the users would not significantly differ. Moreover, Table 3 includes the different simulation parameters used for comparison purposes and the following scenarios. SANOCO-D2D is compared against standalone NOMA with optimal user pairing [6] and OMA scheme in the time domain without D2D communication capabilities between the UEs. In the NOMA satellite transmission, perfect SIC at the strong user is assumed. Furthermore, different operating frequencies for satellite and D2D links are considered. The strong user transmits the decoded signal of the weak user through the entire duration of the time-slot and the time for decoding and re-encoding of the weak user's signal is considered to be negligible.

Table 2. Loo's model's channel parameters and average range D between the LEO satellite and UE for different elevation angles and channel states.

E°	Line-of-Sight			Intermediate Shadow			Deep Shadow			D (km)
	M (dB)	Σ (dB)	MP (dB)	M (dB)	Σ (dB)	MP (dB)	M (dB)	Σ (dB)	MP (dB)	
10°	-0.7	1.9	-38.3	-18.4	8.6	-14.7	-24.4	9.4	-23.9	2300
20°	0.7	2.1	-25.5	-10.0	4.9	-23.3	-25.3	7.0	-26.5	1700
40°	-0.2	1.0	-32.9	-8.6	3.8	-16.1	-15.1	2.6	-16	1000
60°	0.1	1.9	-27.2	-6.9	2.2	-18.6	-13.1	4.2	-19.7	900

Table 3. Simulation parameters.

Simulated frames	100,000
Number of UEs N	32
Region of interest circle radius R	500 m
Satellite downlink frequency f_s	1.625 GHz
D2D operating frequency f_d	2 GHz
Satellite Tx antenna gain G_t^s	24 dBi
Satellite transmit SNR	0–30 dB
UE satellite Rx antenna gain G_r^s	2.7 dBi
System receiver noise temperature T_s	25.7 dBK
UE transmit SNR and P_d	23 dBm and 0.1995 Watt
System receiver noise temperature T_d	24.6 dBK
D2D Tx/Rx antenna gain G_g^d with $g = \{t, r\}$	0 dBi
D2D pathloss model	$127 + 30 \log_{10}(d)$
D2D log-normal shadowing	8 dB
Satellite Bandwidth B_s	5 MHz
UE speed	3 km/hr
Maximum Doppler Shift	40 kHz
Terrestrial Environment	Urban

We define the cases of weak channel (WC), medium channel (MC) and strong channel (SC) users regarding the satellite link. In WC, LoS fading is generated using the parameters presented in Table 2 for the deep shadow state based on the value of the elevation angle. Accordingly, for the SC and MC, UE fading is generated using the parameters of the LoS and intermediate shadow state, respectively and for different elevation angle values. Additionally, as presented in Table 2, based on the elevation angle value and independently of the UE channel state, an average range D in km between the satellite and each UE is considered.

In order to provide performance comparisons among the different schemes, two scenarios are considered. The first scenario focuses on a network within a circular region of interest with radius $R = 500$ m, consisting of a total number of users $N = 32$ uniformly distributed, having an elevation angle equal to 10° , with 50% of users experiencing WC conditions, 37.5% SC and 12.5% MC and different values towards the available terrestrial bandwidth B_d . Then, the second scenario consists of a network within a circular region of interest with $R = 500$ m, a total number of users $N = 32$ uniformly distributed in the region of interest, having an elevation angle equal to 10° , with 50% of users experiencing WC conditions and 50% SC, for different values for the available terrestrial bandwidth B_d .

In Figure 4, the spectral efficiency performance for scenario 1 is presented for different schemes. It can be observed that in the range of 0–26 dB regarding the satellite transmit SNR value, the proposed technique for $B_d = 0.4$ MHz achieves better results than any other value of B_d , and compared to the conventional OMA and NOMA. For SNR values greater than 26 dB, NOMA and SANOCO-D2D with $B_d = 0.1$ MHz achieve slightly better results with almost identical performance. Specifically, for low to medium SNR values, SANOCO-D2D with $B_d = 0.4$ MHz outperforms NOMA. Therefore, the value of 0.4 MHz for the terrestrial D2D link is near the optimal value in order to achieve high spectral efficiency. For terrestrial bandwidth values less than 0.4 MHz, the spectral efficiency of SANOCO-D2D is close to that of NOMA. On the other hand, for $B_d > 0.4$ MHz, because there is no need for extra bandwidth, spectral efficiency starts to decrease, and this claim can be verified by (14) which states that the rate

of the weak user is always limited by the decoding rate of its signal at the strong user. In addition, SANOCO-D2D with $B_d = 0.8$ MHz and $B_d = 1.2$ MHz behave similarly to the case of $B_d = 0.1$ MHz. When the terrestrial bandwidth value is below $B_d = 0.4$ MHz, spectral efficiency degradation is observed, since the weak user chooses to be served directly from the satellite, as the small bandwidth decreases the rate of the D2D channel; i.e., $R_i^{D2D(i,j)} \leq R_i^{DECODED(i,j)}$. In the case where the terrestrial bandwidth value is slightly above $B_d = 0.4$ MHz, the use of extra bandwidth reduces the spectral efficiency performance, and in particular for high SNR, NOMA exhibits superior performance.

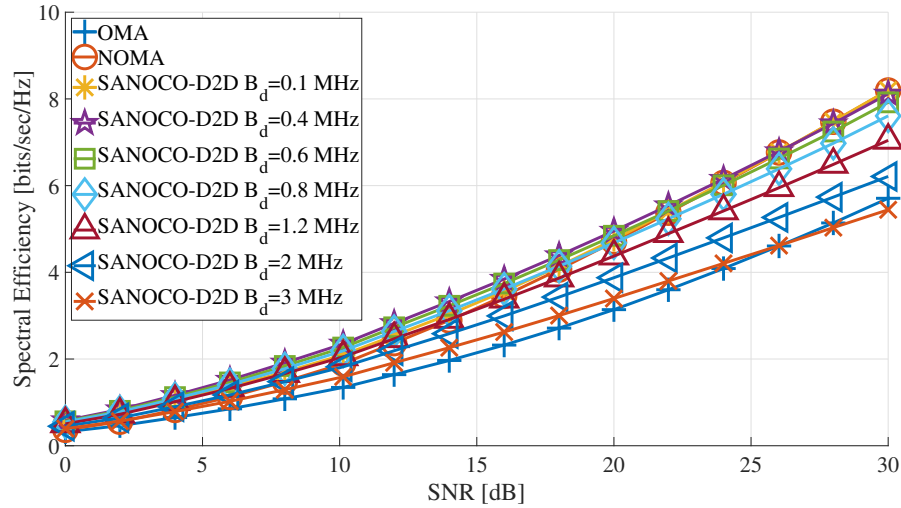


Figure 4. Spectral efficiency for scenario 1, $E = 10^\circ$ and different terrestrial D2D bandwidth values.

In Figure 5 the sum rate performance for scenario 1 is presented. It can be easily observed that independently of the terrestrial bandwidth value, SANOCO-D2D outperforms OMA and NOMA. In greater detail, for $B_d = 0.1$ MHz, SANOCO-D2D behaves better for low to medium SNR values, while for high SNR, its sum rate is slightly better than that of NOMA. This can be attributed to the small terrestrial bandwidth at high SNR values, leading the weak user to prefer the satellite channel for receiving its signal. At low and medium SNR values, the sum rate of SANOCO-D2D is approximately the same for any value of $B_d > 0.4$ MHz. This is justified by considering (14) which highlights the fact that there is no need to allocate additional bandwidth for D2D cooperation. For SNR values above 14 dB, SANOCO-D2D with $B_d = 0.4$ MHz achieves a slightly smaller sum rate than the higher values of B_d , as the decoding rate at the strong user is higher than the rate of the D2D link, and so, a small extra bandwidth is needed for optimal sum rate performance. For example, when $B_d = 0.6$ MHz, at high SNR, the sum rate surpasses that of $B_d = 0.4$ MHz. Thus, it is recommended to use a D2D bandwidth value within $0.4 < B_d < 0.6$, as the adoption of B_d values above 0.6 MHz significantly wastes spectral resources.

Hence, from Figures 4 and 5 it is concluded that dynamic bandwidth allocation for the D2D out-band communication is necessary, in order to optimize both the sum rate and the spectral efficiency performance.

In Figure 6 the spectral efficiency for scenario 1, with $B_d = 0.4$ MHz and different elevation angle values is illustrated for SANOCO-D2D and NOMA. It can be easily observed that for low and medium SNR values and for any value of the elevation angle, the spectral efficiency of SANOCO-D2D outperforms that of NOMA. Specifically, at low and medium SNR values and for $E = 10^\circ$ and $E = 20^\circ$, SANOCO-D2D is superior to NOMA. At high SNR, SANOCO-D2D behaves marginally worse, compared to NOMA in terms of spectral efficiency. Similarly, at low SNR and $E = 40^\circ$ and $E = 60^\circ$, SANOCO-D2D behaves better than NOMA. For medium and high SNR values, the difference in performance becomes negligible. An interesting point in this comparison is that for fairly low SNR

values, the spectral efficiency of SANOCO-D2D with $E = 40^\circ$ is slightly better than that of NOMA technique with $E = 60^\circ$.

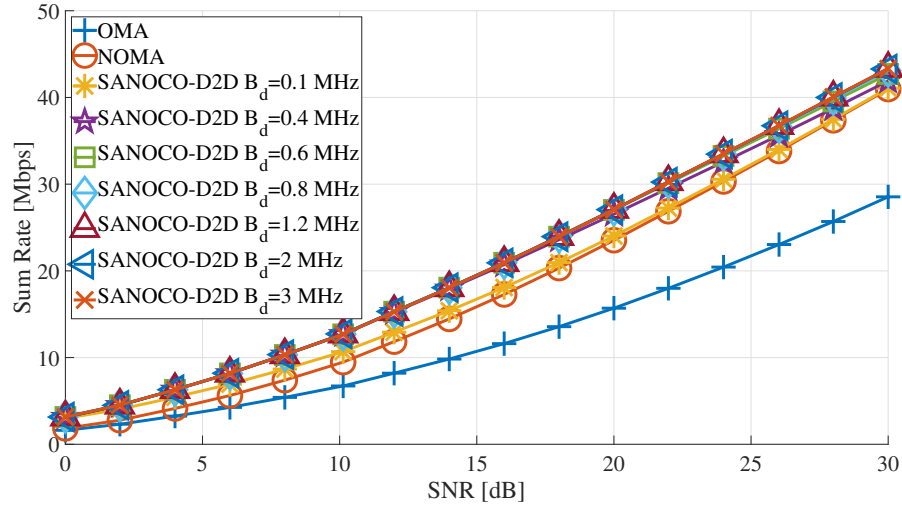


Figure 5. Sum rate for scenario 1, $E = 10^\circ$ and different terrestrial D2D bandwidth values.

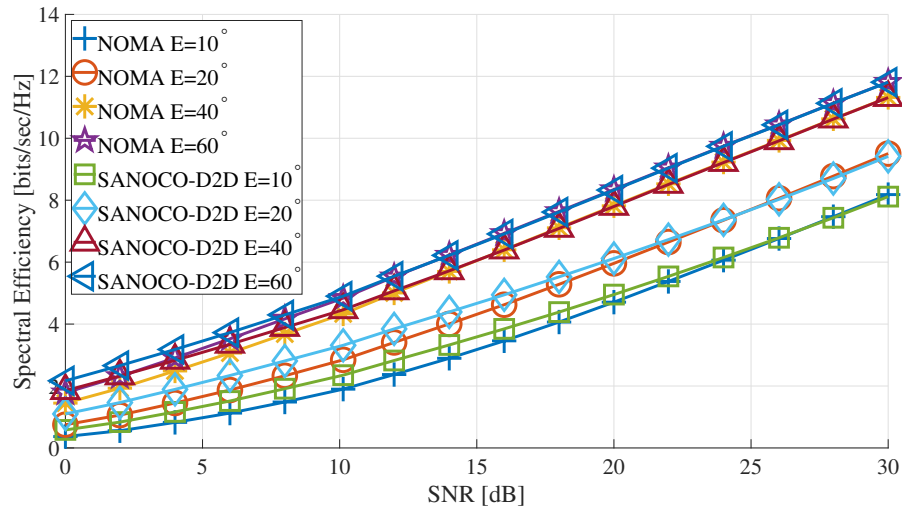


Figure 6. Spectral efficiency for scenario 1, $B_d = 0.4$ MHz and different elevation angle values.

In Figure 7, the sum rate performance for scenario 1, $B_d = 0.4$ MHz and different elevation angle values is presented for SANOCO-D2D and NOMA. It can be seen that throughout the SNR range and independently of the elevation angle value, the sum rate of SANOCO-D2D is better than that of NOMA. In greater detail, for $E = 10^\circ$ and $E = 20^\circ$, SANOCO-D2D outperforms NOMA, and in particular, at low SNR the sum rate of SANOCO-D2D with $E = 10^\circ$ is closer to the sum rate of NOMA with $E = 20^\circ$. The interesting point here is that the sum rate of SANOCO-D2D with $E = 40^\circ$ is better than that of NOMA with $E = 60^\circ$ for SNR values until approximately 7 dB. For high SNR values and $E = 40^\circ$ or $E = 60^\circ$, the sum rate performance of SANOCO-D2D and NOMA is almost identical.

Hence, from Figures 6 and 7, it can be concluded that SANOCO-D2D with appropriately selected terrestrial bandwidth surpasses the performance of NOMA, especially under unfavorable channel conditions, encountered in low and medium transmit SNR values and elevation angles.

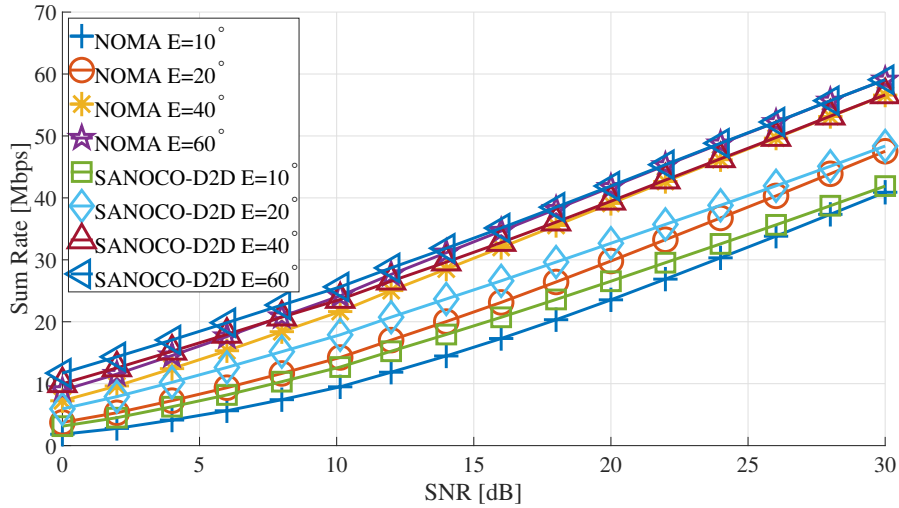


Figure 7. Sum rate for scenario 1, $B_d = 0.4$ MHz and different elevation angle values.

In Figure 8, the spectral efficiency performance for scenario 2 is depicted for different schemes. Firstly, it can be observed that the spectral efficiency of scenario 2 is higher than that of scenario 1. This is justified by considering the lack of users in intermediate channel conditions and the equal percentages of SC and WC users. Thus, depending on the terrestrial channel conditions, each SC user will be paired with a WC user, significantly benefiting the performance of NOMA in the satellite link. Again, SANOCO-D2D with $B_d = 0.4$ MHz achieves better results than any other value of B_d , compared to OMA and NOMA, for an SNR range of 0–26 dB. On the contrary, for SNR values above 26 dB, NOMA and SANOCO-D2D with $B_d = 0.1$ MHz, achieve slightly better results. In general, we can see similar behavior to that of scenario 1, and more specifically, the spectral efficiency performance of SANOCO-D2D for $B_d > 0.4$ MHz (i.e., $B_d = 0.6$ MHz or $B_d = 0.8$ MHz) is slightly improved, since more SC users exist, leading to higher rates from the satellite, thereby leading to an improved usage of the terrestrial bandwidth. This applies to the whole range of transmit SNR but can be perceived at medium and high SNR values. The same is true for the case of $B_d = 0.4$ MHz for the whole range of different transmit SNR values. Furthermore, for $B_d < 0.4$ MHz, e.g., $B_d = 0.1$ MHz, results in an almost identical spectral efficiency to NOMA. This is attributed to the increased number of SC users who achieve higher rates and are able to better assist the weak users. However, usually, a $B_d = 0.1$ limits the rate of the weak users while cooperating with the strong users.

Next, Figure 9 shows the sum rate performance for scenario 2. As it was the case in scenario 1, SANOCO-D2D outperforms OMA and NOMA for any B_d value. Moreover, the sum rate in scenario 2 is higher than that of scenario 1, due to the number of SC users, being equal to that of WC users, thereby improving the performance of NOMA in the satellite. Regarding OMA, as the number of SC users is increased, its total sum rate of the system increases. Furthermore, SANOCO-D2D with $B_d \geq 0.4$ MHz offers better results than NOMA. For $B_d < 0.4$ MHz, as it is the case of $B_d = 0.1$ MHz this increase is significantly smaller, because the allocated D2D bandwidth limits the transmission rate of the strong user. It should be noted that compared to scenario 1, the sum rate in scenario 2 using SANOCO-D2D with $B_d > 0.4$ MHz starts to increase at approximately 10 dB, faster than scenario 1. As illustrated in Figure 9, a significant increase in the value of B_d cannot offer much higher sum rate, and causes a significant decrease in the spectral efficiency, as presented in Figure 8, because the strong user decoding rate is the upper bound for the weak user rate, of the D2D link's achievable rate. Thus, dynamic bandwidth allocation is needed, in order to achieve a balance between sum rate and spectral efficiency performance.

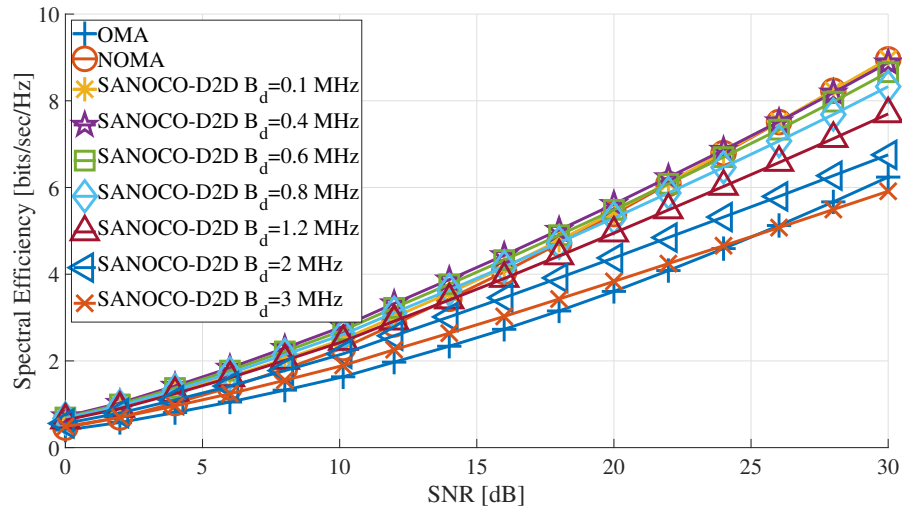


Figure 8. Spectral efficiency for scenario 2, $E = 10^\circ$ and different terrestrial D2D bandwidth values.

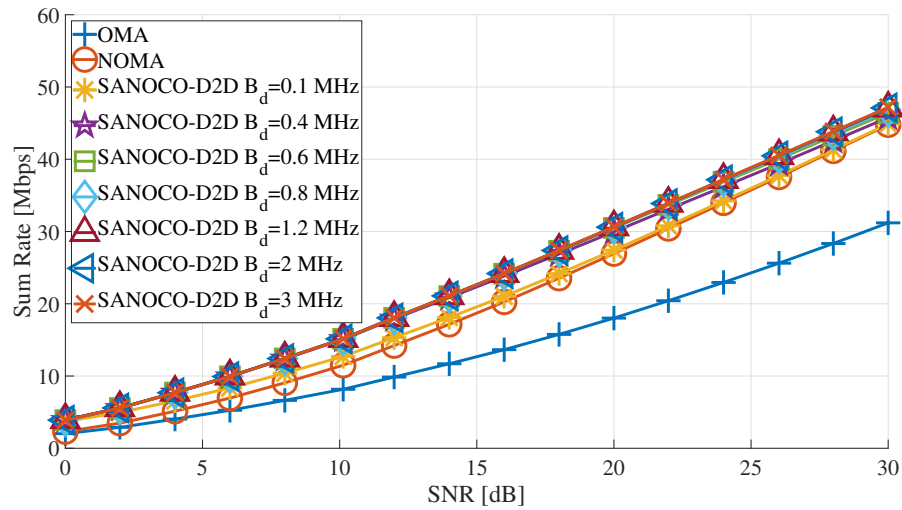


Figure 9. Sum rate for scenario 2, $E = 10^\circ$ and different terrestrial D2D bandwidth values.

The final comparisons for scenario 2 are depicted in Figures 10 and 11. In greater detail, the spectral efficiency and sum rate performance, with $B_d = 0.4$ MHz and different values of elevation angle is evaluated. Regarding the spectral efficiency, similarly to scenario 1, for low and medium transmit SNR values and any elevation angle, SANOCO-D2D exhibits better performance than NOMA. Then, for higher SNR and equal elevation angles, SANOCO-D2D behaves slightly worse than NOMA. Furthermore, at low SNR and $E = 40^\circ$ or $E = 60^\circ$, SANOCO-D2D offers improved spectral efficiency, compared to NOMA. For medium and high SNR, differences for the two schemes are quite small. Next, the sum rate comparison outlines that for any SNR and elevation angle value, SANOCO-D2D performs better than NOMA. Moreover, the sum rate of SANOCO-D2D with $E = 40^\circ$ is higher than that of NOMA with $E = 60^\circ$ for SNR values approximately up to 8 dB, due to the increased number of SC users. Finally, for high SNR values with $E = 40^\circ$ or $E = 60^\circ$, the sum rate results of SANOCO-D2D and NOMA are almost identical.

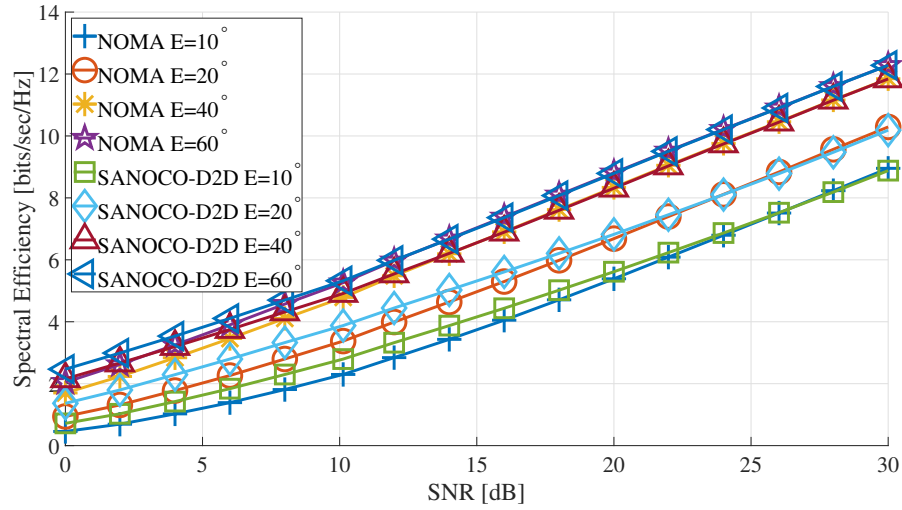


Figure 10. Spectral efficiency efficiency for scenario 2, $B_d = 0.4$ MHz and different elevation angle values.

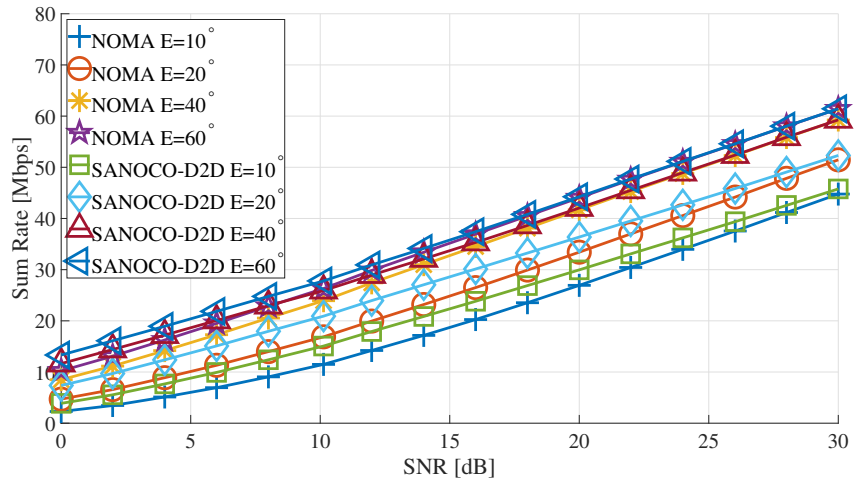


Figure 11. Sum rate for scenario 2, $B_d = 0.4$ MHz and different elevation angle values.

Overall, the sum rate results of SANOCO-D2D in both scenarios show that achievable rate of the weak user can be significantly improved. This gain stems from the fact that the strong users cooperate with the weak users in the system through out-band D2D communication. In this way, fairness in the system is ensured as a more homogeneous QoS is achieved throughout the satellite's coverage area. In addition, the simultaneous out-band satellite transmission and D2D cooperation reduce the delay inherent to two-hop transmissions and the increased sum rate allows more packets to be served, thereby benefiting further performance metrics, such as the average packet delay.

Finally, Table 4 summarizes the key characteristics of the proposed scheme and the scheme of [6]. It can be observed that the addition of D2D cooperation improves the overall performance of the wireless transmission at an affordable complexity.

Table 4. Comparative table regarding the key characteristics of the SANOCO-D2D and the scheme of [6].

	SANOCO-D2D	NOMA Scheme [6]
Complexity	Medium	Low
D2D Cooperation	Yes	No
Relaying Mode	Half Duplex	N/A
CSI Overhead	Medium	Low
Power Allocation	Optimal	Optimal
Dynamic D2D Channel Bandwidth	Yes	N/A
Reliability	High	Medium
Spectral Efficiency	High	Medium
Sum Rate	High	Medium
Fairness	High	Low

5. Conclusions

The integration of satellite segments to terrestrial wireless networks has been shown to facilitate the provision of massive connectivity to coexisting users and devices. At the same time, incorporating efficient non-orthogonal multiple access, in terms of wireless resource utilization can guarantee fairness and system capacity. In this context, SANOCO-D2D, a satellite-aided NOMA cooperative D2D scheme was presented for integrated terrestrial satellite networks. Through SANOCO-D2D, the sum rate of the system was improved for different channel conditions, and it was shown that under a properly selected value for the terrestrial bandwidth, enhanced spectral efficiency, compared to standalone NOMA and OMA can be achieved, especially for low and medium transmit SNR. SANOCO-D2D offers increased QoS homogeneity through proper power allocation depending on the channel asymmetry between the strong and weak users and the possibility for simultaneous out-band D2D cooperation, using the strong users as relays. As a result, the fairness in the system is improved and at the same time, leveraging the increased sum rate, more packets are served, leading to a reduction of the total delay.

Integrated satellite-terrestrial networks provide a fertile research field and there are several future directions that can expand this work. Given the various benefits of SANOCO-D2D, a distributed weighted matching algorithm could be adopted in order to further decrease the computational complexity and achieve workload sharing between the nodes of the network [29]. Recently, the adoption of artificial intelligence and machine learning has been a driving force towards fully autonomous zero-touch wireless networks [30,31]. SANOCO-D2D can adopt different learning techniques to reduce the complexity of user pairing and channel state information acquisition and processing. Another important technique that should be studied is full-duplex communication, either in-band or out-band where dynamic bandwidth allocation should be optimized in the device-to-device link. There have been several full-duplex cooperative transmission schemes that can be integrated in SANOCO-D2D, incorporating successive transmissions by the source and relay nodes [32,33] or full-duplex reception and transmission from a single node [34]. Finally, the issue of outdated CSI represents another important future direction for this work, since in practical systems, the acquired CSI of a link might be different from the actual one, due to delays generated by the feedback mechanism [35,36].

Author Contributions: Conceptualization, M.K., N.N. and D.V.; methodology, M.K. and N.N.; software, M.K.; validation, M.K., N.N. and D.V.; formal analysis, M.K.; investigation, M.K. and N.N.; writing—original draft preparation, M.K. and N.N.; writing—review and editing, N.N. and D.V.; supervision, D.V. All authors have read and agreed to the published version of the manuscript.

Funding: This research received no external funding.

Conflicts of Interest: The authors declare no conflict of interest.

Acknowledgments: The research work was supported by the Hellenic Foundation for Research and Innovation (HFRI) under the HFRI PhD Fellowship grant (Fellowship Number: 1507).

Abbreviations

The following abbreviations are used in this manuscript:

5G	Fifth Generation
AWGN	Additive White Gaussian Noise
BS	Base Station
C-NOMA	Cooperative NOMA
CSI	Channel State Information
D2D	Device-to-Device
FSL	Free Space Pathloss
GEO	Geosynchronous Earth Orbit
IoT	Internet of Things
LEO	Low Earth Orbit
LMS	Land Mobile Satellite
LoS	Line of Sight
MC	Medium Channel
MEO	Medium Earth Orbit
MP	Multipath Component
NOMA	Non-Orthogonal Multiple Access
OMA	Orthogonal Multiple Access
QoS	Quality-of-Service
SANOCO-D2D	Satellite-Aided NOMA with Cooperative D2D Communication
SC	Strong Channel
SIC	Successive Interference Cancellation
SNR	Signal-to-Noise Ratio
TDMA	Time-Division Multiple Access
UE	User Equipment
WC	Weak Channel

References

1. Liu, J.; Shi, Y.; Fadlullah, Z.M.; Kato, N. Space-Air-Ground Integrated Network: A Survey. *IEEE Commun. Surv. Tutor.* **2018**, *20*, 2714–2741. [[CrossRef](#)]
2. Michailidis, E.T.; Nomikos, N.; Bithas, P.S.; Vouyioukas, D.; Kanatas, A.G. Optimal 3-D Aerial Relay Placement for Multi-User MIMO Communications. *IEEE Trans. Aerosp. Electron. Syst.* **2019**, *55*, 3218–3229. [[CrossRef](#)]
3. Di, B.; Song, L.; Li, Y.; Poor, H.V. Ultra-Dense LEO: Integration of Satellite Access Networks into 5G and Beyond. *IEEE Wirel. Commun.* **2019**, *26*, 62–69. [[CrossRef](#)]
4. Ding, Z.; Liu, Y.; Choi, J.; Sun, Q.; Elkashlann, M.; Chih-Lin, I.; Poor, H.V. Application of Non-Orthogonal Multiple Access in LTE and 5G Networks. *IEEE Commun. Mag.* **2017**, *55*, 185–191. [[CrossRef](#)]
5. Ding, Z.; Lei, X.; Karagiannidis, G.K.; Schober, R. Yuan, J.; Bhargava, V.K. A Survey on Non-Orthogonal Multiple Access for 5G Networks: Research Challenges and Future Trends. *IEEE J. Sel. Areas Commun.* **2017**, *35*, 2181–2195. [[CrossRef](#)]
6. Zhu, L.; Zhang, J.; Xiao, Z.; Cao, X.; Wu, D.O. Optimal User Pairing for Downlink Non-Orthogonal Multiple Access (NOMA). *IEEE Wirel. Commun. Lett.* **2019**, *8*, 328–331. [[CrossRef](#)]
7. Nomikos, N.; Charalambous, T.; Vouyioukas, D.; Karagiannidis, G.K.; Wichman, R. Hybrid NOMA/OMA with Buffer-Aided Relay Selection in Cooperative Networks. *IEEE J. Sel. Top. Signal Process.* **2019**, *13*, 524–537. [[CrossRef](#)]
8. Yan, X.; An, K.; Liang, T.; Zheng, G.; Ding, Z.; Chatzinotas, S.; Liu, Y. The Application of Power-Domain Non-Orthogonal Multiple Access in Satellite Communication Networks. *IEEE Access* **2019**, *7*, 63531–63539. [[CrossRef](#)]
9. Zhu, X.; Jiang, C.; Kuang, L.; Ge, N.; Lu, J. Non-Orthogonal Multiple Access Based Integrated Terrestrial-Satellite Networks. *IEEE J. Sel. Areas Commun.* **2017**, *35*, 2253–2267. [[CrossRef](#)]
10. Yan, X.; Xiao, H.; Wang, C.; An, K.; Chronopoulos, A.T.; Zheng, G. Performance Analysis of NOMA-Based Land Mobile Satellite Networks. *IEEE Access* **2018**, *6*, 31327–31339. [[CrossRef](#)]
11. Yan, X.; Xiao, H.; An, K.; Zheng, G.; Tao, W. Hybrid Satellite Terrestrial Relay Networks With Cooperative Non-Orthogonal Multiple Access. *IEEE Commun. Lett.* **2018**, *22*, 978–981. [[CrossRef](#)]

12. Dun, H.; Ye, F.; Jiao, S.; Liu, D. Power Control for Device-to-Device Communication with a Hybrid Relay Mode in Unequal Transmission Slots. *Electronics* **2018**, *7*, 17. [[CrossRef](#)]
13. Penda, D.D.; Nomikos, N.; Charalambous, T.; Johansson, M. Minimum Power Scheduling under Rician Fading in Full-Duplex Relay-Assisted D2D Communications. In Proceedings of the IEEE GLOBECOM 2017 Workshops: Workshop on Full-Duplex Communications for Future Wireless Networks, Singapore, 4–8 December 2017.
14. Gür, G. Spectrum Sharing and Content-Centric Operation for 5G Hybrid Satellite Networks: Prospects and Challenges for Space-Terrestrial System Integration. *IEEE Veh. Technol. Mag.* **2019**, *14*, 38–48. [[CrossRef](#)]
15. Di, B.; Zhang, H.; Song, L.; Li, Y.; Li, G.Y. Ultra-Dense LEO: Integrating Terrestrial-Satellite Networks Into 5G and Beyond for Data Offloading. *IEEE Trans. Wirel. Commun.* **2019**, *18*, 47–62. [[CrossRef](#)]
16. Yan, X.; Xiao, H.; Wang, C.; An, K. Outage Performance of NOMA-Based Hybrid Satellite-Terrestrial Relay Networks. *IEEE Wirel. Commun. Lett.* **2018**, *7*, 538–541. [[CrossRef](#)]
17. FCC, OneWeb Non-Geostationary Satellite System (Attachment A). 2016. Available online: http://licensing.fcc.gov/myibfs/download.do?attachment_key=1190495 (accessed on 4 September 2020)
18. FCC, SpaceX Non-Geostationary Satellite System (Attachment A). 2016. Available online: https://licensing.fcc.gov/myibfs/download.do?attachment_key=1252848 (accessed on 4 September 2020)
19. Loo, C. A Statistical Model for a Land Mobile Satellite Link. *IEEE Trans. Veh. Technol.* **1985**, *34*, 122–127.
20. Jakes, W.C. *Microwave Mobile Communication*; John Wiley & Sons, Ltd.: Hoboken, NJ, USA, 1974.
21. 3GPP. Evolved Universal Terrestrial Radio Access (E-UTRA); Further Advancements for E-UTRA Physical Layer Aspects. TR 36.814. V9.0.0. 3rd Generation Partnership Project (3GPP). 2010. Available online: <http://www.3gpp.org/ftp/Specs/html-info/36814.htm> (accessed on 4 September 2020).
22. Edmonds, J. Maximum matching and a polyhedron with 0,1-vertices. *J. Res. Natl. Bur. Stand. Sect. B* **1969**, *69*, 125–130. [[CrossRef](#)]
23. Gabow, H.N. *Implementation of Algorithms for Maximum Matching on Nonbipartite Graphs*; Department of Computer Science, Stanford University: Stanford, CA, USA, 1973.
24. Lawler, E.L. *Combinatorial Optimization: Networks and Matroids*; Holt, Rinehart and Winston: New York, NY, USA, 1976.
25. Galil, Z.; Micali, S.; Gabow, H. An O($\text{EV} \log V$) Algorithm for Finding a Maximal Weighted Matching in General Graphs. *SIAM J. Comput.* **1986**, *15*, 120–130. [[CrossRef](#)]
26. Library of Efficient Models and Optimization in Networks. Available online: <http://lemon.cs.elte.hu/pub/doc/latest-svn/a00388.html> (accessed on 4 September 2020).
27. Fontan, F.P. Vazquez-Castro, M. Cabado, C.E. Garcia, J.P. Kubista. E. Statistical Modeling of the LMS Channel. *IEEE Trans. Veh. Technol.* **2001**, *50*, 1549–1567. [[CrossRef](#)]
28. Fontán, F.P.; Espíñeira, P.M. The Land Mobile Satellite Channel. In *Modelling the Wireless Propagation Channel: A simulation approach with Matlab*; Wiley: Hoboken, NJ, USA, 2008, 213–227.
29. Wattenhofer, R. Distributed Weighted Matching. In *Distributed Computing*; Springer: Berlin/Heidelberg, Germany, **2004**, 335–348.
30. Kato, N.; Md Fadlullah, Z.; Tang, F.; Mao, B.; Tani, S.; Okamura, A.; Liu, J. Optimizing Space-Air-Ground Integrated Networks by Artificial Intelligence. *IEEE Wirel. Commun.* **2019**, *26*, 140–147. [[CrossRef](#)]
31. Bithas, P.S.; Michailidis, E.T.; Nomikos, N.; Vouyioukas, D.; Kanatas, A.G. A Survey on Machine-Learning Techniques for UAV-Based Communications. *Sensors* **2019**, *19*, 5170. [[CrossRef](#)] [[PubMed](#)]
32. Liau, Q.Y.; Leow, C.Y.; Ding, Z. Amplify-and-Forward Virtual Full-Duplex Relaying-Based Cooperative NOMA. *IEEE Wirel. Commun. Lett.* **2018**, *7*, 464–467. [[CrossRef](#)]
33. Nomikos, N.; Charalambous, T.; Pappas, N.; Vouyioukas, D.; Wichman, R. LoLA4SOR: A Low-Latency Algorithm for Successive Opportunistic Relaying. In Proceedings of the IEEE International Conference on Computer Communications: Workshop on Ultra-Low Latency in Wireless Networks (ULLWN), Paris, France, 29 April–2 May 2019.
34. Nomikos, N.; Charalambous, T.; Vouyioukas, D.; Wichman, R.; Karagiannidis, G.K. Integrating Broadcasting and NOMA in Full-Duplex Buffer-Aided Opportunistic Relay Networks. *IEEE Trans. Veh. Technol.* **2020**, *69*, 9157–9162. [[CrossRef](#)]

35. Vicario, J.L.; Bel, A.; Lopez-Salcedo, J.A.; Seco, G. Opportunistic Relay Selection with Outdated CSI: Outage Probability and Diversity Analysis. *IEEE Trans. Wirel. Commun.* **2009**, *8*, 2872–2876. [[CrossRef](#)]
36. Islam, T.; Michalopoulos, D.S.; Schober, R.; Bhargava, V.K. Buffer-Aided Relaying with Outdated CSI. *IEEE Trans. Wirel. Commun.* **2016**, *15*, 1979–1997. [[CrossRef](#)]



© 2020 by the authors. Licensee MDPI, Basel, Switzerland. This article is an open access article distributed under the terms and conditions of the Creative Commons Attribution (CC BY) license (<http://creativecommons.org/licenses/by/4.0/>).